Condensation vs phase ordering in the dynamics of first-order transitions

C. Castellano,[1,*] F. Corberi,[1,2,†] and M. Zannetti[1,‡]
[1]*Istituto Nazionale di Fisica della Materia, Unità di Salerno and Dipartimento di Fisica, Università di Salerno, 84081 Baronissi, Salerno, Italy*
[2]*Dipartimento di Scienze Fisiche, Università di Napoli, Mostra d'Oltremare, Padiglione 19, 80125 Napoli, Italy*
(Received 27 March 1997)

The origin of the noncommutativity of the limits $t\to\infty$ and $N\to\infty$ in the dynamics of first-order transitions is investigated. In the large-N model, i.e., $N\to\infty$ taken first, the low-temperature phase is characterized by condensation of the large-wavelength fluctuations rather than by genuine phase ordering as when $t\to\infty$ is taken first. A detailed study of the scaling properties of the structure factor in the large-N model is carried out for quenches above, at, and below T_c. Preasymptotic scaling is found and crossover phenomena are related to the existence of components in the order parameter with different scaling properties. Implications for phase ordering in realistic systems are discussed. [S1063-651X(97)01010-6]

PACS number(s): 64.60.Ak, 05.70.Fh, 64.60.My, 64.75.+g

I. INTRODUCTION

The large-time behavior of a system quenched at or below the critical point is characterized by scale invariance [1]. For the equal time structure factor one has

$$C(\vec{k},t)=L^{\alpha}(t)F(kL(t)), \tag{1}$$

where

$$L(t)\sim t^{1/z} \tag{2}$$

is the characteristic length growing with time according to a power law and $F(x)$ is the scaling function. The physics behind Eq. (1) is quite simple and is basically due to the degeneracy of the low-temperature state. After the quench an exponentially fast process takes place leading to local equilibrium. If multiple choice is available, correlated regions of the possible low-temperature phases are formed. From that point onward equilibration proceeds through the coarsening of these correlated regions, whose characteristic size $L(t)$ grows according to Eq. (2). The difference between quenches to T_c and below T_c is that in the first case the correlated regions are fractal (Appendix A), while in the second case they are compact. Apart from this, in both cases the equilibration process becomes slow (if the system is infinite, equilibrium is never reached) and after domains of the ordered phases have formed, scaling behavior occurs since the residual time dependence is confined in the typical size $L(t)$ of the correlated regions.

The whole time evolution can be divided into a preasymptotic and an asymptotic regime, with a smooth transition between the two. The asymptotic regime displays universality and is controlled by a fixed-point structure. The universality classes are determined by features such as the presence or absence of a conservation law, the number N of components of the order parameter, the dimensionality d of space, and the final temperature T_F of the quench. More precisely, on the temperature axis there is an unstable fixed point at the critical temperature T_c and an attractive fixed point at $T_F=0$. For the exponent α one has

$$\alpha=\begin{cases}2-\eta & \text{for } T_F=T_c\\ d & \text{for } T_F<T_c,\end{cases} \tag{3}$$

where η is the usual exponent of the static critical phenomena. The exponent z coincides with the exponent of the dynamical critical phenomena for $T_F=T_c$. Instead, for any final temperature below T_c, $z=2$ for a nonconserved order parameter (NCOP), while for a conserved order parameter (COP) $z=3$ when $N=1$ and $z=4$ when $N>1$. The scaling function $F(x)$ also displays universal features and is sensitive to the space dimensionality through the presence ($N<d$) or absence ($N>d$) of localized topological defects. By contrast, in the preasymptotic regime the evolution of the system is not universal, as it depends on the initial conditions of the quench and on the actual value of the final temperature.

A complete theory of the process then should derive the scaling behavior from the basic equation of motion for the order parameter and should be able to describe how the relatively simple universal asymptotic regime emerges out of the complexity of the preasymptotic regime. Ideally, one would like to have a manageable reference theory that accounts, at least qualitatively, for the basic features of the process and a systematic procedure for the computation of the corrections [2]. A scheme of this type is available for quenches to T_c, where, despite the difficulty due to the lack of time translational invariance, the field theoretical machinery developed for critical phenomena is to a large extent applicable [3]. Instead, for quenches below T_c the present status of theoretical understanding is far from this standard. What we have in this case is the linear theory [4] for the very early stage of the process, which applies only when initial conditions are so small that it is actually justified to employ a linear approximation, and *ad hoc* late-stage theories [5]. Although these late-stage theories have had much success in the computation of the scaling functions, they are based on uncontrolled ap-

*Electronic address: castellano@na.infn.it
†Electronic address: corberi@na.infn.it
‡Electronic address: zannetti@na.infn.it

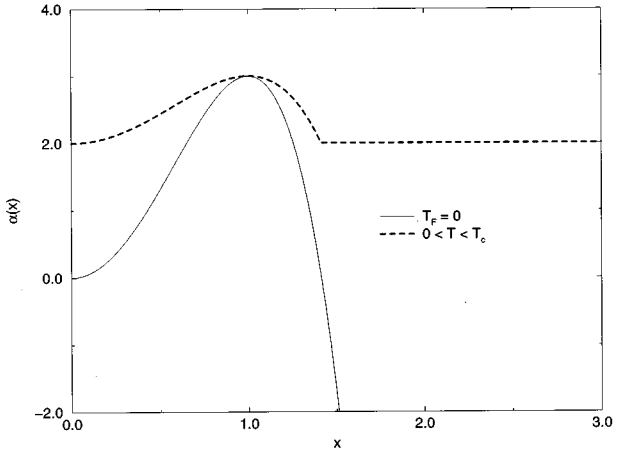

FIG. 1. Spectrum of the multiscaling exponent $\alpha(x)$ for quenches with a COP and $d=3$.

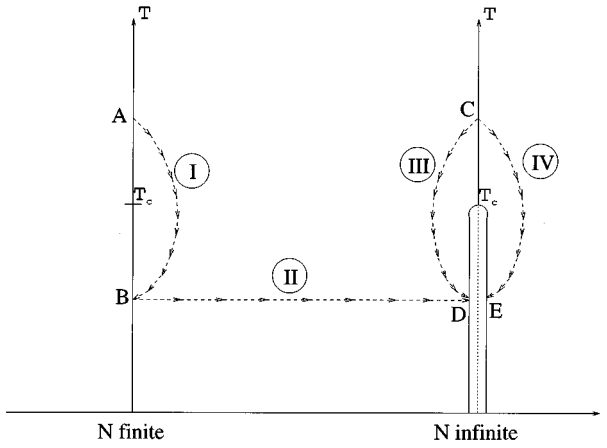

FIG. 2. Schematic representation of the relaxation processes in the systems with N finite and $N=\infty$.

proximations. Furthermore, the late-stage theories do not connect to the early-stage theory, if this is available at all. So there is no theoretical understanding of the complex phenomenology arising at the breakdown of the early-stage theory and leading to the onset of scaling [6]. Proposals for the systematic improvement of the late-stage theory have been put forth [7], but as of now a first-principles theory of phase-ordering processes is out of reach.

In this theoretical landscape a special position is occupied by the $1/N$ expansion. As applied to critical phenomena, this technique provides a very clear instance of what is to be understood for a systematic theory: There is a lowest-order analytically tractable approximation (the large-N model) that captures the basic physics and there is an expansion parameter $(1/N)$ that allows for the systematic computation of the corrections. The scheme applies successfully also to quenches to the critical point [3] and, at first sight, it would seem to be applicable as well to the phase-ordering processes. Indeed, in the large-N model one can solve exactly [8] for the structure factor and one finds that the standard scaling form (1) is obeyed for long times with a NCOP [9]. In particular one finds $z=2$ and α is given by Eq. (3) with $\eta=0$. The scaling functions can also be found explicitly [10]. It is to be stressed that in the solution of the model with $N=\infty$ there are no *ad hoc* hypotheses and the above outlined picture of the asymptotic behavior with scaling, universality, and temperature fixed points is derived from the solution of the equation of motion.

However, when the model is solved with a COP [8,10], although the form (1) is obeyed with $\alpha=2$ and $z=4$ for $T_F=T_c$, for the quenches to $T_F<T_c$ the more general multiscaling form

$$C(\vec{k},t)\sim[L(k_mL)^{(2-d)/d}]^{\alpha(x)}F(x) \tag{4}$$

is found, where $L(t)\sim t^{1/4}$, $k_m(t)$ is the peak wave vector, and $x=k/k_m$. The exponent $\alpha(x)$ is given by

$$\alpha(x)=q+\varrho\,\varphi(x), \tag{5}$$

with

$$q=\begin{cases}2 & \text{for } 0<T_F<T_c\\ 0 & \text{for } T_F=0,\end{cases} \tag{6}$$

$$\varrho=\begin{cases}d-2 & \text{for } 0<T_F<T_c\\ d & \text{for } T_F=0.\end{cases} \tag{7}$$

Furthermore, when $0<T_F<T_c$ the function $\varphi(x)$ in Eq. (5) is given by

$$\varphi(x)=\begin{cases}\psi(x) & \text{for } x<x^*\\ 0 & \text{for } x>x^*,\end{cases} \tag{8}$$

with $x^*=\sqrt{2}$ and

$$\psi(x)=1-(1-x^2)^2, \tag{9}$$

while $\varphi(x)=\psi(x)$ for all values of x when $T_F=0$. Finally,

$$F(x)=\begin{cases}\dfrac{T_F}{x^2} & \text{for } 0<T_F<T_c\\ 1 & \text{for } T_F=0.\end{cases} \tag{10}$$

Leaving aside for the moment the apparent formal complication of Eqs. (4)–(10), the important feature that is immediately evident is that, contrary to Eq. (3), now there are three distinct asymptotic behaviors for $T_F=T_c$, $0<T_F<T_c$, and $T_F=0$. For $T_F=T_c$ the structure factor obeys standard scaling with $\alpha=2$ as in the NCOP case. Instead, for $T_F<T_c$ the exponent α depends on x (Fig. 1) and the scaling form (4) involves two lengths $k_m^{-1}(t)$ and $L(t)$, which differ by a logarithmic factor [8]

$$(k_mL)^4=\ln L^d+(2-d)\ln(k_mL). \tag{11}$$

The functional form of $\alpha(x)$ is different for $0<T_F<T_c$ and $T_F=0$. This means that $T_F=T_c$ and $T_F=0$ are both unstable fixed points and in between there is a new line of fixed points for $0<T_F<T_c$. The temperature below the critical point is no longer an irrelevant variable.

If the $1/N$ expansion were a good systematic theory, the $1/N$ corrections ought to produce only minor quantitative changes on the picture outlined above. However, this expec-

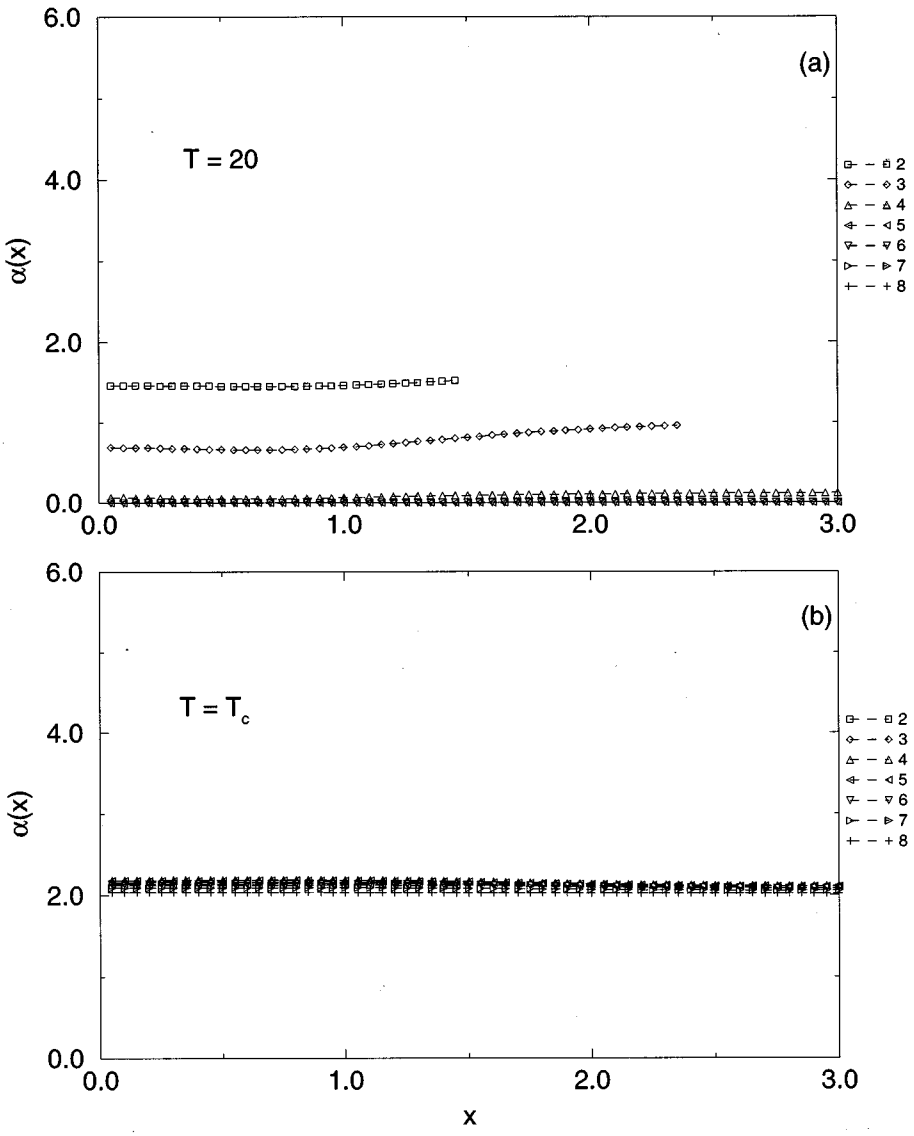

FIG. 3. Evolution of $\alpha(x)$ for a NCOP and $d=3$. (a) $T_F \gg T_c$ and (b) $T_F = T_c$. Different curves refer to a sequence of time intervals growing exponentially with the label. In this and all other figures except Fig. 8, very early times are not shown for simplicity.

tation has not been fulfilled by the work of Bray and Humayun [11], who found that for quenches to $T_F=0$ and a COP standard scaling of the form (1) is restored in systems with any finite value of N. The same result is very likely to apply also to the quenches to $0<T_F<T_c$. Therefore, the main qualitative features emerging in lowest order, such as the multiscaling behavior and the relevance of the temperature fluctuations, are expected to be a peculiarity of the case with N strictly infinite, disappearing as soon as higher-order corrections are taken into account. In other words, the limits $N\to\infty$ and $t\to\infty$ do not commute for quenches to $T_F<T_c$. In this paper we explore in some detail this phenomenon and we clarify what dynamical process is really described when the $N\to\infty$ limit is taken first. This helps to understand what correct use is to be made of the large-N model in this area of nonequilibrium statistical mechanics.

The gross features of what goes on in the quenches below T_c can be described with the help of Fig. 2. The phase-ordering process of a system with finite N is represented by path I connecting the disordered states A to the ordered states B. These latter states are mixtures of broken symmetry states. If *after* equilibrium has been established the $N\to\infty$ limit is taken as depicted by path II, the system is brought into a state D that is the mixture of the $N\to\infty$ limits of each one of the broken symmetry states. If instead the $N\to\infty$ limit is taken *before* the quench, the process starts from a disordered state C of the system with infinitely many components and the ensuing dynamical process does not connect C to D along path III. As a matter of fact, the process depicted by III does not exist. Rather, the dynamical evolution follows path IV leading to low-temperature states E that are quite distinct from D. In other words, the system with $N=\infty$ supports two different low-temperature phases whose realization depends on the order of the limits $t\to\infty$ and $N\to\infty$. The distinction between these two phases is reminiscent of the difference between the zero-field low-temperature states in the spherical model [12] and in the mean spherical model [13]. In particular, states E are very similar to the low-temperature states in

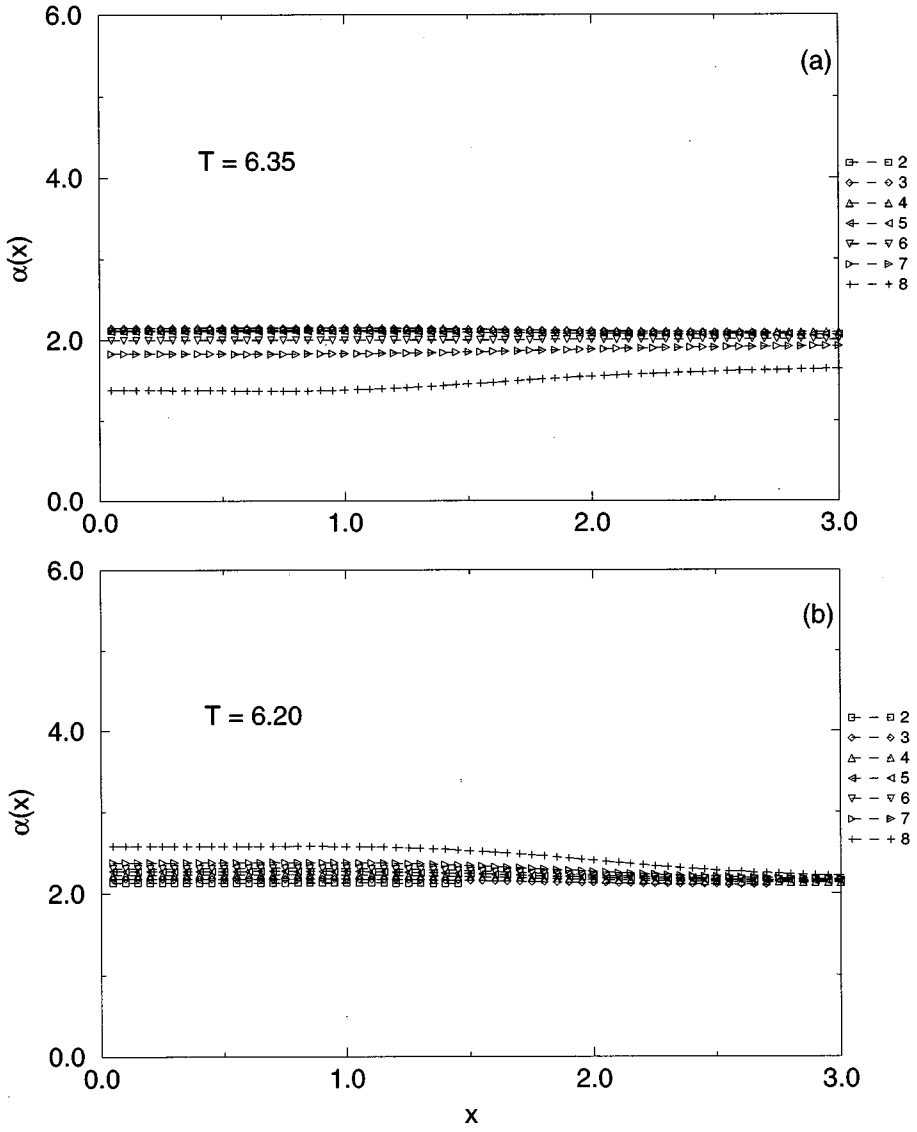

FIG. 4. Evolution of $\alpha(x)$ for a NCOP and $d=3$ for quenches to T_F slightly above and slightly below T_c. Symbols and time intervals are related as in Fig. 3.

the ideal Bose gas, as it will be clarified in Sec. II. The point to be stressed here is that in the static $1/N$ expansion states A and B are reached, respectively, from states C and D, while $1/N$ corrections over states E are not informative on states B. This clarifies why the $1/N$ expansion can be used for quenches to T_c, but not below T_c, *as an approximation for processes with finite* N.

What then is the use of the large-N model for growth kinetics. There is an obvious intrinsic interest once it is clear that even though the model does not describe a phase-ordering process of the usual type, the model is well defined and describes the relaxation across a phase transition. The growth process generated in the time evolution can be studied in detail and produces nontrivial behavior. The outcome is quite interesting since by modulating the initial noise and the final temperature, remarkable crossover phenomena are obtained. Here is where the model gives information also on systems with finite N, even if it is not perturbatively close to the phase-ordering processes. In fact, the phenomenology of the structure factor exhibits features that are also found in the preasymptotic behavior of systems with finite N [14,15]. Therefore, through the large-N model insight can be gained into the very complex time regime preceding the onset of scaling in realistic systems.

The paper is organized as follows. In Sec. II the model is introduced, the noncommutativity of the $t\to\infty$ and $N\to\infty$ limits is clarified, and the nature of the low-temperature phases in the large-N model is investigated. In Sec. III the numerical solution for the structure factor is presented and crossovers between different scaling behaviors are analyzed by means of the multiscaling analysis. Conclusions are presented in Sec. IV.

II. LOW-TEMPERATURE PHASES

In the following we consider the relaxation dynamics of a system with an N-component order parameter $\vec{\phi}(\vec{x})=(\phi_1(\vec{x}),\ldots,\phi_N(\vec{x}))$ that is initially prepared in a high-temperature disordered state and is suddenly quenched to a

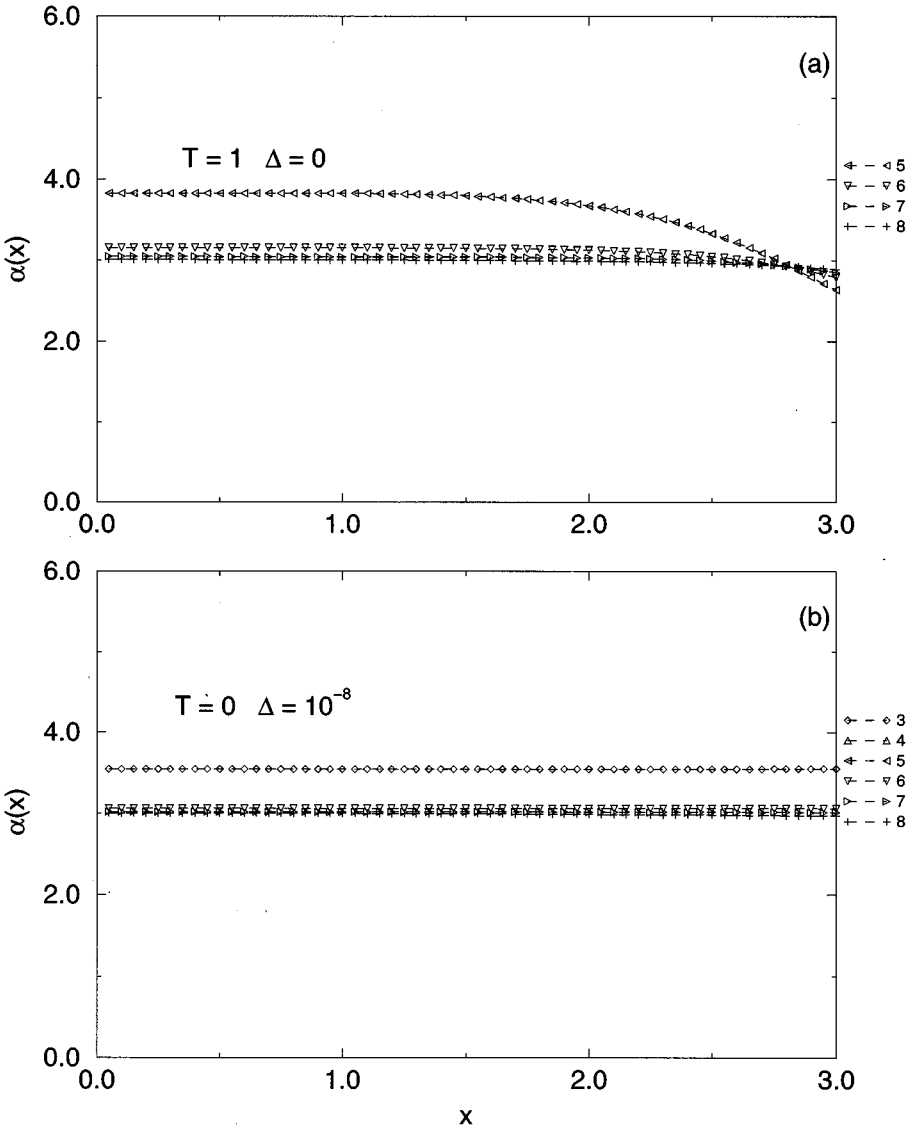

FIG. 5. Evolution of $\alpha(x)$ for a NCOP and $d=3$ for quenches to $0<T_F<T_c$ and $T_F=0$. Symbols and time intervals are related as in Fig. 3.

lower temperature. The evolution of the order parameter is governed by the time-dependent Ginzburg-Landau model

$$\frac{\partial\vec{\phi}(\vec{x},t)}{\partial t}=-(i\nabla)^p\frac{\delta\mathcal{H}[\vec{\phi},N]}{\delta\vec{\phi}(\vec{x})}+\vec{\eta}(\vec{x},t), \tag{12}$$

where $p=0$ for a NCOP, $p=2$ for a COP, and $\vec{\eta}(\vec{x},t)$ is the Gaussian white noise with expectations

$$\langle\vec{\eta}(\vec{x},t)\rangle=0,$$

$$\langle\eta_\alpha(\vec{x},t)\,\eta_\beta(\vec{x}',t')\rangle=2T_F(i\nabla)^p\delta_{\alpha\beta}\delta(\vec{x}-\vec{x}')\,\delta(t-t'). \tag{13}$$

The free-energy functional is of the form

$$\mathcal{H}[\vec{\phi},N]=\int_V d^dx\left[\frac{1}{2}(\nabla\vec{\phi})^2+\frac{r}{2}\vec{\phi}^2+\frac{g}{4N}(\vec{\phi}^2)^2\right], \tag{14}$$

where V is the volume of the system, $r<0$, and $g>0$. The order-parameter probability distribution in the initial state can be taken to be of the form

$$P_0[\vec{\phi},N]=\frac{1}{Z_0}\exp\left\{-\frac{1}{2\Delta}\int d^dx\,\vec{\phi}^2(\vec{x})\right\} \tag{15}$$

describing the absence of correlations at high temperature

$$\langle\phi_\alpha(\vec{x},0)\,\phi_\beta(\vec{x}',0)\rangle=\Delta\,\delta_{\alpha\beta}\delta(\vec{x}-\vec{x}'). \tag{16}$$

As mentioned in the Introduction, if one wants to consider the $N\to\infty$ limit, in order to determine the nature of the final equilibrium state attention must be paid to the order in which the $N\to\infty$ and $t\to\infty$ limits are taken. Let us consider first the sequence $\lim_{N\to\infty}\lim_{t\to\infty}$. Keeping N finite, the equation of motion (12) induces the time evolution of the probability distribution from the initial form (15) toward the Gibbs state

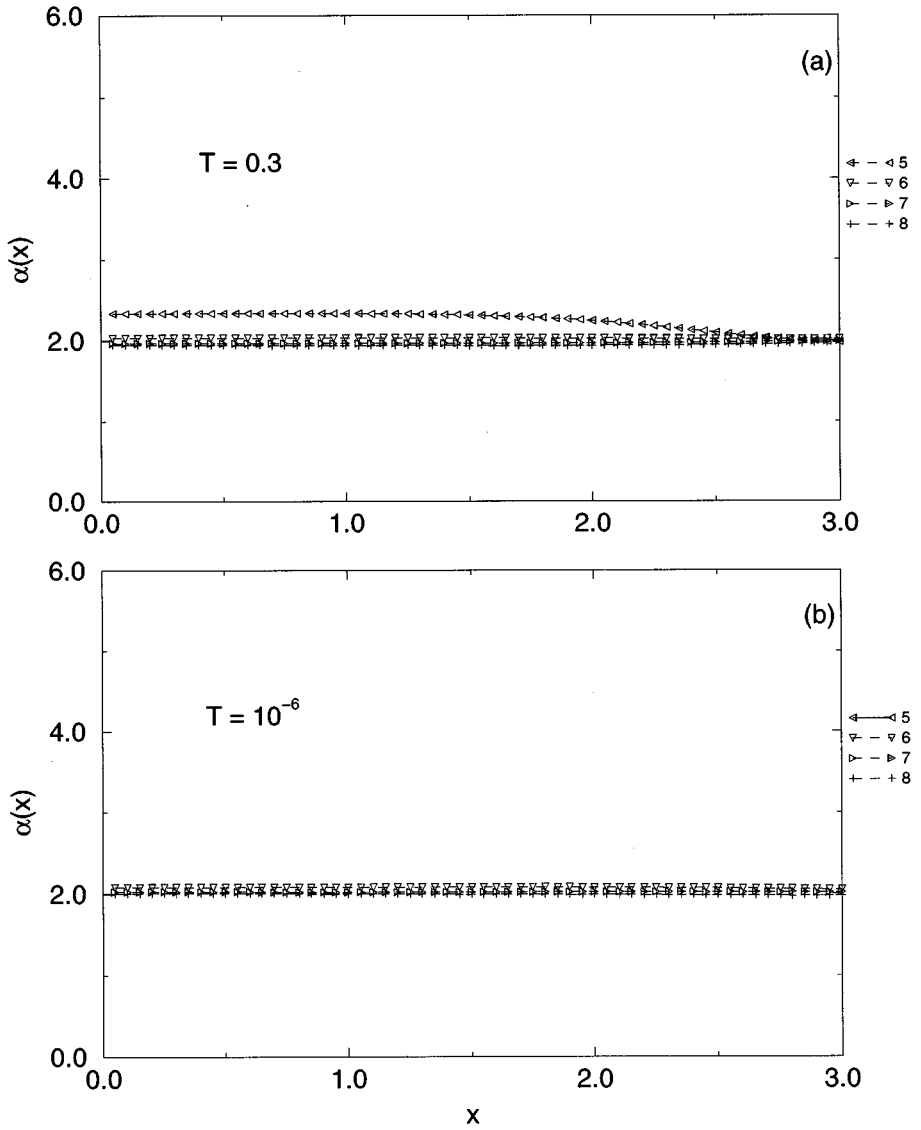

FIG. 6. Evolution of $\alpha(x)$ for a NCOP and $d=2$ for quenches to $T_F=0.3$ and $T_F=10^{-6}$. Symbols and time intervals are related as in Fig. 3.

$$P[\vec{\phi},t,N]\rightarrow P_{eq}[\vec{\phi},N]=\frac{1}{Z}\exp\left\{-\frac{1}{T_F}\mathcal{H}[\vec{\phi},N]\right\}. \quad (17)$$

In the infinite volume limit $P_{eq}[\vec{\phi},N]$ describes a disordered pure state if T_F is above T_c and the $O(N)$ symmetrical mixture of the broken symmetry states if T_F is below T_c. If we now take the $N\rightarrow\infty$ limit (path of type II in Fig. 1), for $T_F\geqslant T_c$ we obtain the pure phase C

$$P_{eq}[\vec{\phi},\infty]=\frac{1}{Z}\exp\left\{-\frac{1}{2T_F}\sum_{\vec{k}}(k^2+r+gS)\vec{\phi}(\vec{k})\cdot\vec{\phi}(-\vec{k})\right\}, \quad (18)$$

where S is given by the self-consistency condition

$$S=\frac{1}{V}\sum_{\vec{k}}\langle\phi_\beta(\vec{k})\phi_\beta(-\vec{k})\rangle \quad (19)$$

and β denotes the generic component. Below T_c, denoting by $\vec{m}$ the expectation value of $\vec{\phi}(\vec{x})$ in the broken-symmetry state, the $N\rightarrow\infty$ limit D of the mixture is obtained

$$P_{eq}[\vec{\phi},\infty]=\int d\vec{m}\,\rho(\vec{m})\mu[\vec{\phi}|\vec{m}], \quad (20)$$

where $\rho(\vec{m})$ is the uniform probability density over the sphere of radius m and the pure state $\mu[\vec{\phi}|\vec{m}]$ is given by

$$\mu[\vec{\phi}|\vec{m}]=\delta[(\vec{\phi}-\vec{m})\cdot\hat{m}]\times\frac{1}{Z}\exp\left\{-\frac{1}{2T_F}\sum_{\vec{k}}(k^2+r+gm^2+gS_\perp)\times\vec{\phi}_\perp(\vec{k})\cdot\vec{\phi}_\perp(-\vec{k})\right\}, \quad (21)$$

where $\vec{\phi}_\perp=\vec{\phi}-(\vec{\phi}\cdot\hat{m})\hat{m}$. The quantities $S_\perp$ and m are determined by the self-consistency relations

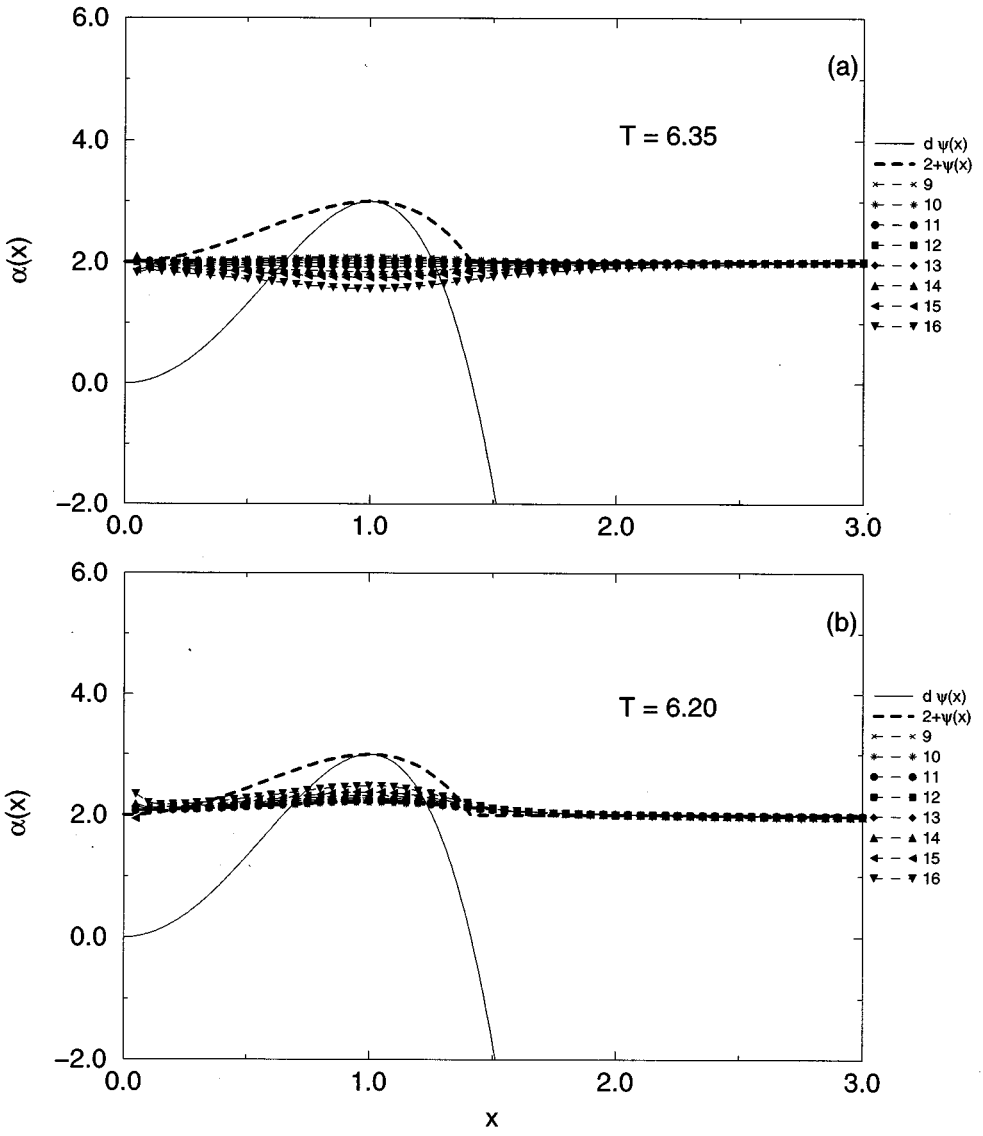

FIG. 7. Evolution of $\alpha(x)$ for a COP and $d=3$ for quenches to T_F slightly above and slightly below T_c. Symbols and time intervals are related as in Fig. 3.

$$S_\perp = \frac{1}{V}\sum_{\vec{k}} \langle \phi_{\perp\beta}(\vec{k})\phi_{\perp\beta}(-\vec{k})\rangle, \tag{22}$$

$$r + g(m^2 + S_\perp) = 0. \tag{23}$$

In the end, computing averages with the weight functions (18) and (20), we find the well-known result of the large-N model

$$\langle \phi_\beta(\vec{k})\phi_\beta(-\vec{k})\rangle = \begin{cases} \dfrac{T_F}{k^2 + r + gS} & \text{for } T_F \geq T_c \\ \dfrac{T_F}{k^2} + m^2\delta(\vec{k}) & \text{for } T_F < T_c \end{cases} \tag{24}$$

for the equilibrium structure factor in states C and D. The average value of the order parameter is given by

$$m^2 = -\frac{r}{g}\left(\frac{T_c - T_F}{T_c}\right), \tag{25}$$

with

$$T_c = -\frac{r(d-2)}{gK_d\Lambda^{d-2}}, \tag{26}$$

where Λ is a wave-vector cutoff and $K_d = [2^{d-1}\pi^{d/2}\Gamma(d/2)]^{-1}$. The $\delta(\vec{k})$ term appearing in Eq. (24), below T_c, is the Bragg peak due to ordering in the low-temperature phase D.

Let us now consider the limits in the opposite order. Taking the $N\to\infty$ limit at the outset amounts to taking the limit on the equation of motion (12), which becomes effectively linearized

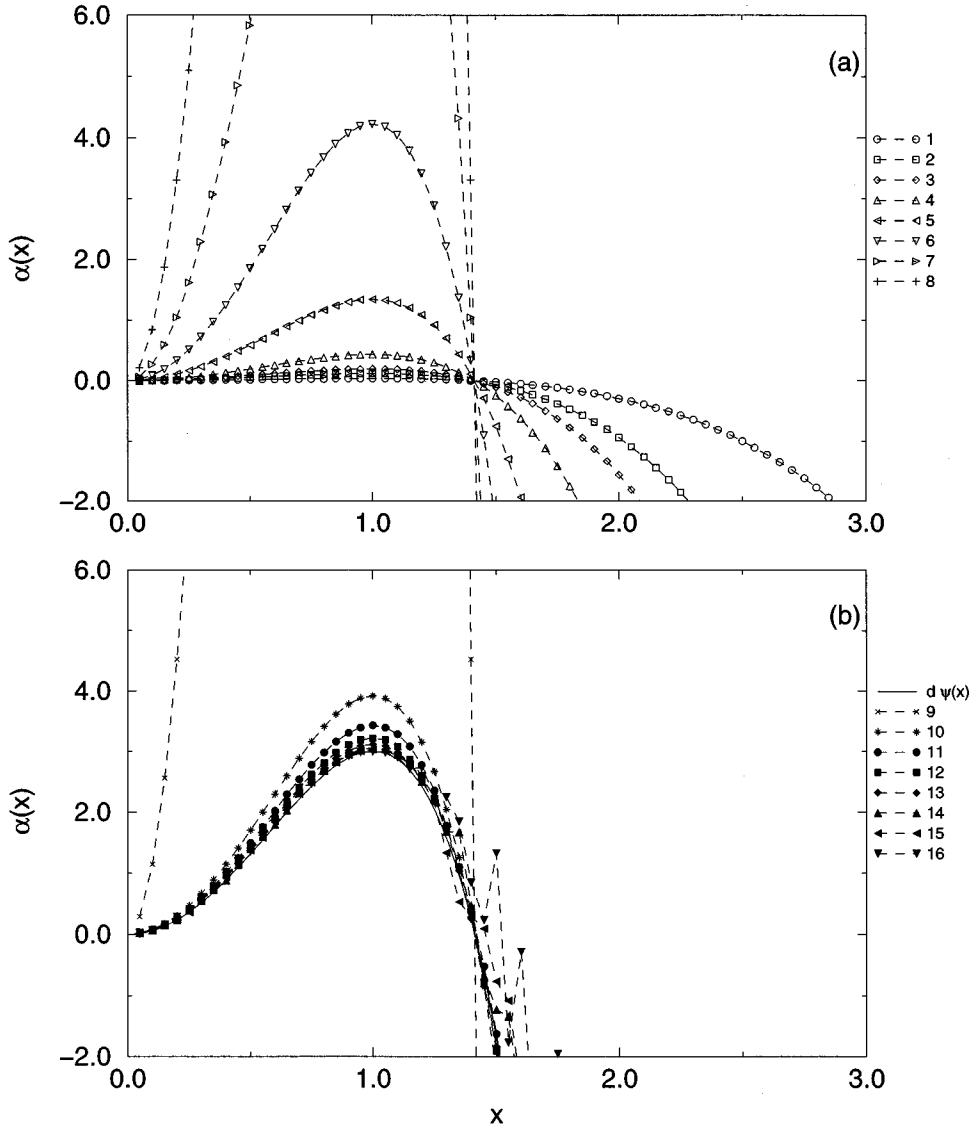

FIG. 8. Evolution of $\alpha(x)$ for a COP and $d=3$ for a quench to $T_F=0$: (a) early times and (b) intermediate to late times. Different curves refer to a sequence of time intervals growing exponentially with the label.

$$\frac{\partial \phi_\beta(\vec{k},t)}{\partial t} = -k^p[k^2+R(t)]\phi_\beta(\vec{k},t)+\vec{\eta}_\beta(\vec{k},t), \quad (27)$$

with

$$R(t)=r+gS(t) \quad (28)$$

and

$$S(t)=\frac{1}{V}\sum_{\vec{k}} \langle \phi_\beta(\vec{k},t)\phi_\beta(-\vec{k},t)\rangle. \quad (29)$$

Due to the linearity of Eq. (27), the time-dependent probability distribution is Gaussian

$$P[\vec{\phi},t,\infty]=\frac{1}{Z(t)}\exp\left\{-\frac{1}{2}\sum_{\vec{k}} C^{-1}(\vec{k},t)\vec{\phi}(\vec{k})\cdot\vec{\phi}(-\vec{k})\right\}, \quad (30)$$

with

$$C(\vec{k},t)=\langle \phi_\beta(\vec{k},t)\phi_\beta(-\vec{k},t)\rangle. \quad (31)$$

Taking next the $t\to\infty$ limit

$$P[\vec{\phi},t,\infty]\to Q_{eq}[\vec{\phi},\infty] = \frac{1}{Z}\exp\left\{-\frac{1}{2}\sum_{\vec{k}} C_{eq}^{-1}(\vec{k})\vec{\phi}(\vec{k})\cdot\vec{\phi}(-\vec{k})\right\}, \quad (32)$$

we obtain a Gaussian state for any final temperature and it is legitimate to ask whether there is still a phase transition.

From Eq. (27) it is straightforward to obtain [10] the equation of motion for the structure factor

$$\frac{\partial C(\vec{k},t)}{\partial t} = -2k^p[k^2+R(t)]C(\vec{k},t)+2k^pT_F, \quad (33)$$

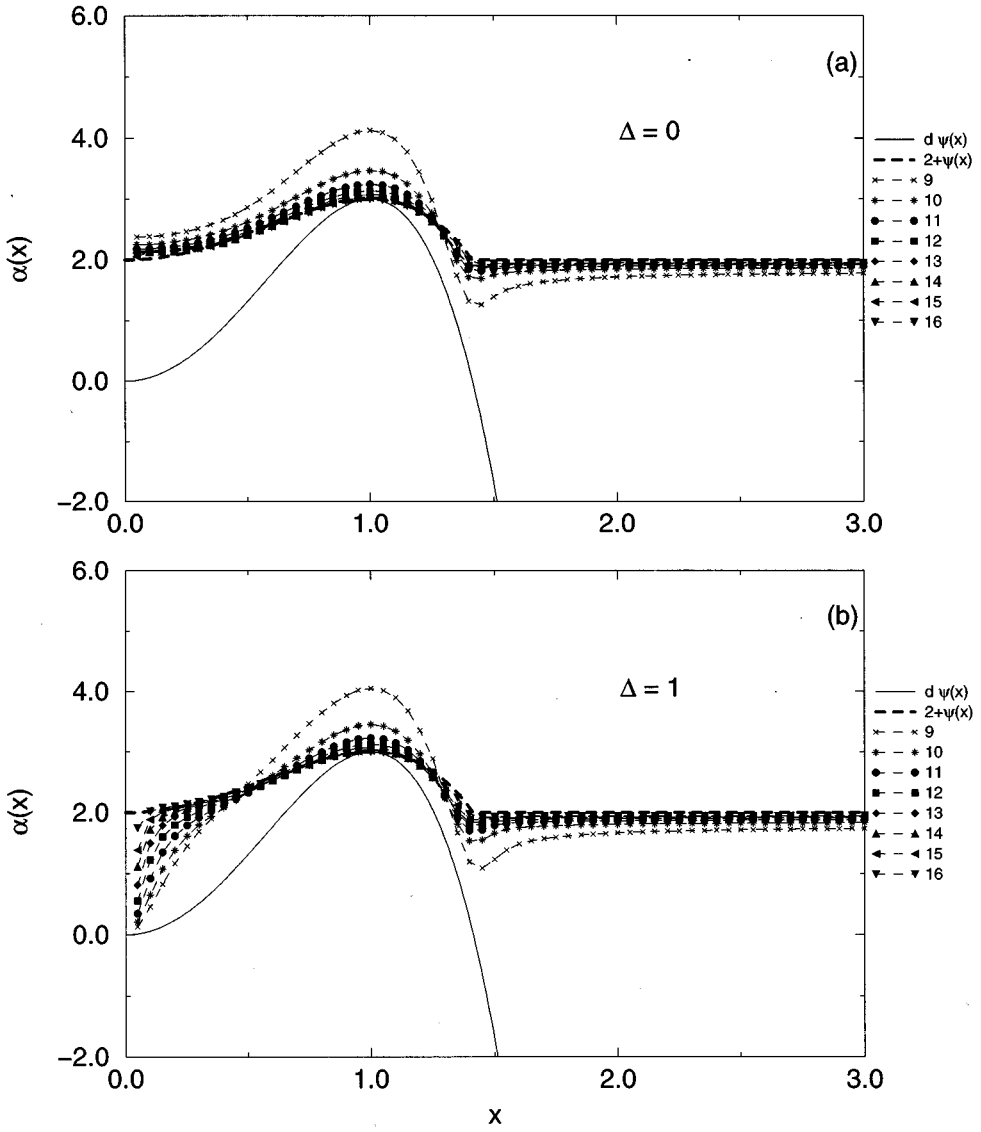

FIG. 9. Evolution of $\alpha(x)$ for a COP, $d=3$, and $T_F=1$: (a) zero initial fluctuations and (b) large initial fluctuations. Symbols and time intervals are related as in Fig. 3.

which, after equilibration is reached, yields

$$C_{eq}(\vec{k})=\frac{T_F}{k^2+\xi^{-2}} \tag{34}$$

with a NCOP and

$$C_{eq}(\vec{k})=\begin{cases} C(\vec{k}=0,t=0) & \text{for } \vec{k}=0 \\ \dfrac{T_F}{k^2+\xi^{-2}} & \text{for } \vec{k}\neq 0 \end{cases} \tag{35}$$

with a COP, where $\lim_{t\to\infty}R(t)=\xi^{-2}$ is the inverse square equilibrium correlation length. From Eq. (28)

$$\xi^{-2}=r+\frac{gT_F}{V}\sum_{\vec{k}}\frac{1}{k^2+\xi^{-2}}, \tag{36}$$

where the sum extends over all values of $\vec{k}$ for a NCOP and over $\vec{k}\neq 0$ for a COP. We now analyze Eq. (36) in the NCOP case, referring to Appendix B for the modifications in the argument required by the conservation law. With V finite the solution of Eq. (36) for ξ is finite for any temperature. As expected, there is no phase transition in a finite volume system. In the infinite volume limit Eq. (36) becomes

$$\xi^{-2}=r+gT_FB(\xi^{-2})+\frac{gT_F}{V\xi^{-2}}, \tag{37}$$

where the function $B(x)$, defined by

$$B(x)=\int\frac{d^dk}{(2\pi)^d}\frac{1}{k^2+x}, \tag{38}$$

is a monotonical decreasing function of x with a maximum value at $B(0)=K_d\Lambda^{d-2}/(d-2)$. In writing Eq. (37) the $\vec{k}=\vec{0}$ contribution to the sum (36) has been explicitly sepa-

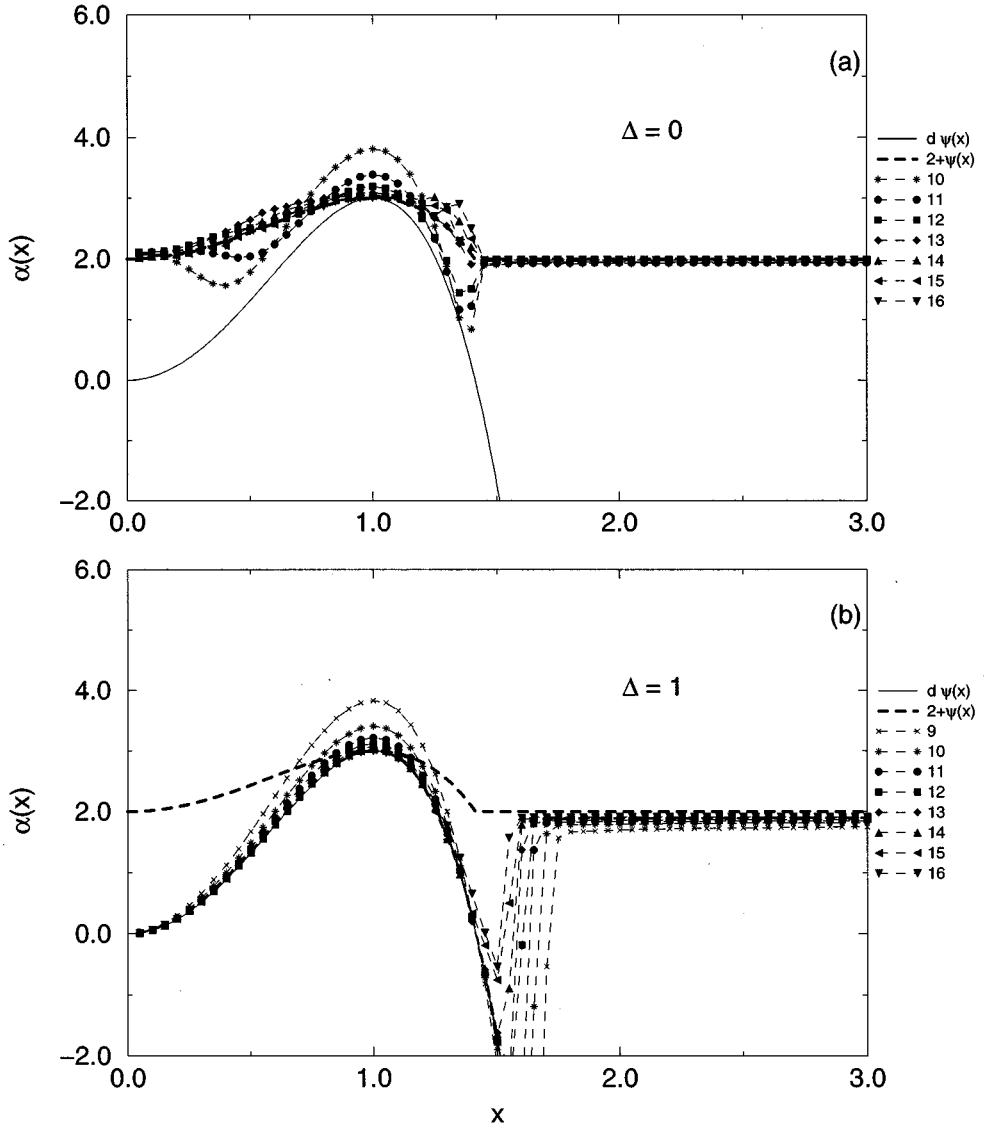

FIG. 10. Evolution of $\alpha(x)$ for a COP, $d=3$, and $T_F=10^{-6}$: (a) zero initial fluctuations and (b) large initial fluctuations. Symbols and time intervals are related as in Fig. 3.

rated out. Defining $\gamma^2=T_F/V\xi^{-2}$ and introducing the temperature $T_c=-r/gB(0)$, which coincides with Eq. (26), Eq. (37) can be rewritten as

$$\frac{1}{g}\xi^{-2}=\left[\frac{r}{g}\left(\frac{T_c-T_F}{T_c}\right)+\gamma^2\right]+T_F[B(\xi^{-2})-B(0)], \quad (39)$$

with the solution (Appendix B)

$$\begin{aligned} &\xi^{-2}>0, \quad \gamma^2=0 \quad \text{for } T_F>T_c, \\ &\xi^{-2}=0, \quad \gamma^2=0 \quad \text{for } T_F=T_c, \\ &\xi^{-2}=0, \quad \gamma^2=-r/g\left(\frac{T_c-T_F}{T_c}\right) \text{ for } T_F<T_c, \end{aligned} \quad (40)$$

which shows the existence of the phase transition at T_c. For the structure factor this implies

$$C_{eq}(\vec{k})=\begin{cases} \dfrac{T_F}{k^2+\xi^{-2}}, & T_F\geqslant T_c \\ \dfrac{T_F}{k^2}+\gamma^2\delta(\vec{k}), & T_F<T_c, \end{cases} \quad (41)$$

and taking into account the form (40) of γ^2, Eq. (41) is identical to Eq. (24). Thus, as far as the structure factor is concerned, the same result is found irrespective of the order of the limits $t\to\infty$ and $N\to\infty$. However, comparing the states, $Q_{eq}[\vec{\phi},\infty]$ coincides with $P_{eq}[\vec{\phi},\infty]$ above T_c, but not below, where

$$Q_{eq}[\vec{\phi},\infty]=\frac{1}{\sqrt{2\pi\gamma^2 V}}\exp\left\{-\frac{\phi^2(0)}{2\gamma^2 V}\right\} \times\frac{1}{Z}\exp\left\{-\frac{1}{2}\sum_{k\neq 0} C_{eq}^{-1}(\vec{k})\,\vec{\phi}(\vec{k})\cdot\vec{\phi}(-\vec{k})\right\}. \quad (42)$$

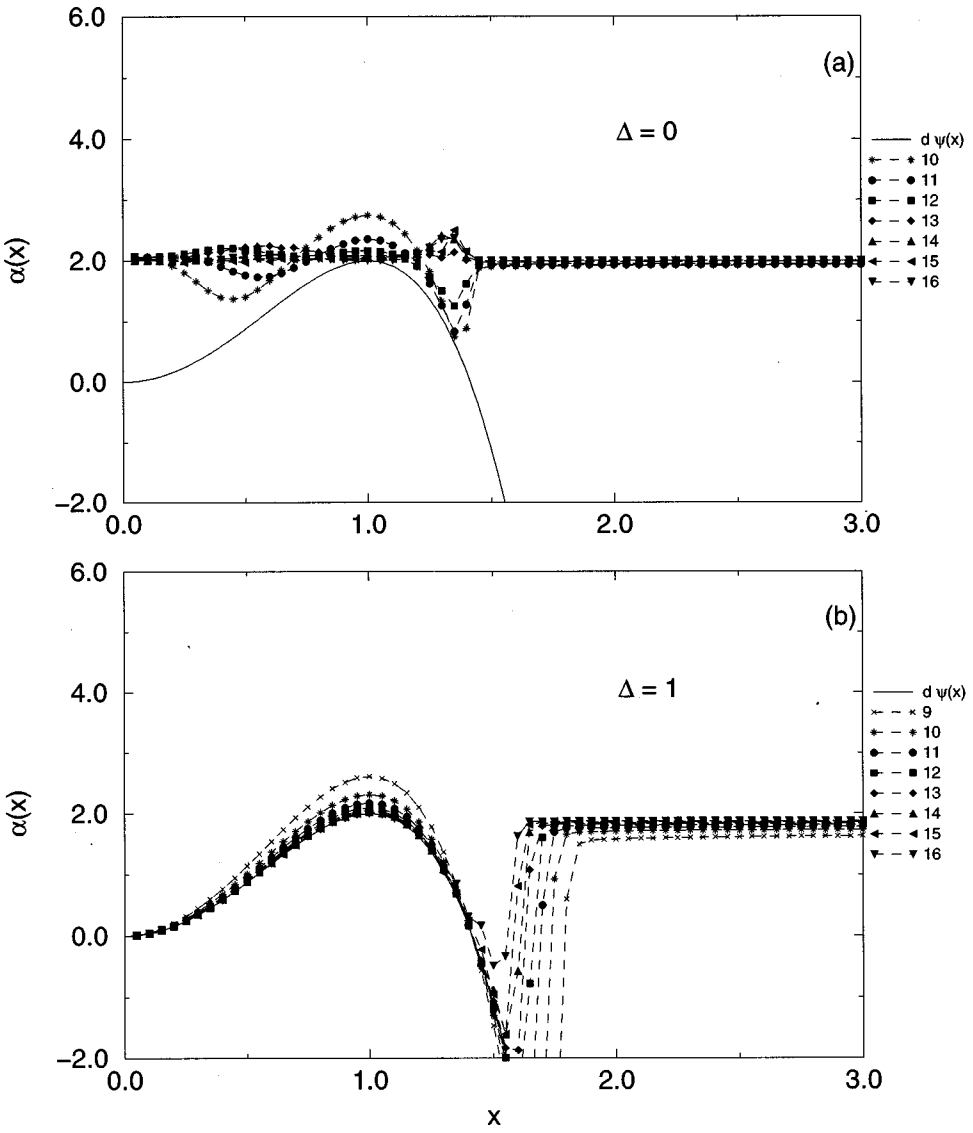

FIG. 11. Evolution of $\alpha(x)$ for a COP, $d=2$, and $T_F=10^{-6}$: (a) zero initial fluctuations and (b) large initial fluctuations. Symbols and time intervals are related as in Fig. 3.

This is a state exactly of the same form as the zero-field low-temperature state in the mean spherical model, while state D is a mixture as in the spherical model [16].

Thus, despite the formal similarity, the Bragg peaks in Eqs. (24) and (41) have different physical meanings. In the former case, it signals the formation of a mixture of ordered states, while in the latter it is due to the macroscopic growth of the $\vec{k}=\vec{0}$ term in the sum (36). What we have here is a low-temperature phase obtained by condensation of the fluctuations at $\vec{k}=\vec{0}$, as in the ideal Bose gas, with $C_{eq}(\vec{k}=\vec{0})$ playing the role of the zero-momentum occupation number.

Finally, notice that with $d=2$ the critical temperature (26) vanishes. Hence all states with $T_F>0$ are disordered states and the limits $t\to\infty$ and $N\to\infty$ commute for the quenches to any finite final temperature. Conversely, $T_F=0$ is not a critical temperature; rather it is an ordering temperature. Therefore, the quench to $T_F=0$ is an ordering process and the limits are not supposed to commute in this case.

III. SCALING BEHAVIORS

In this section we investigate the time evolution of the structure factor by solving numerically the equation of motion (33). It is convenient to comment beforehand on the structure of this solution. Integrating Eq. (33), the structure factor can be written as the sum of two contributions

$$C(\vec{k},t)=C_0(\vec{k},t)+C_T(\vec{k},t), \tag{43}$$

with

$$C_0(\vec{k},t)=\Delta\exp\left\{-2k^p\int_0^t ds[k^2+R(s)]\right\} \tag{44}$$

and

$$C_T(\vec{k},t)=2T_Fk^p\int_0^t dt'\exp\left\{-2k^p\int_{t'}^t ds[k^2+R(s)]\right\}. \tag{45}$$

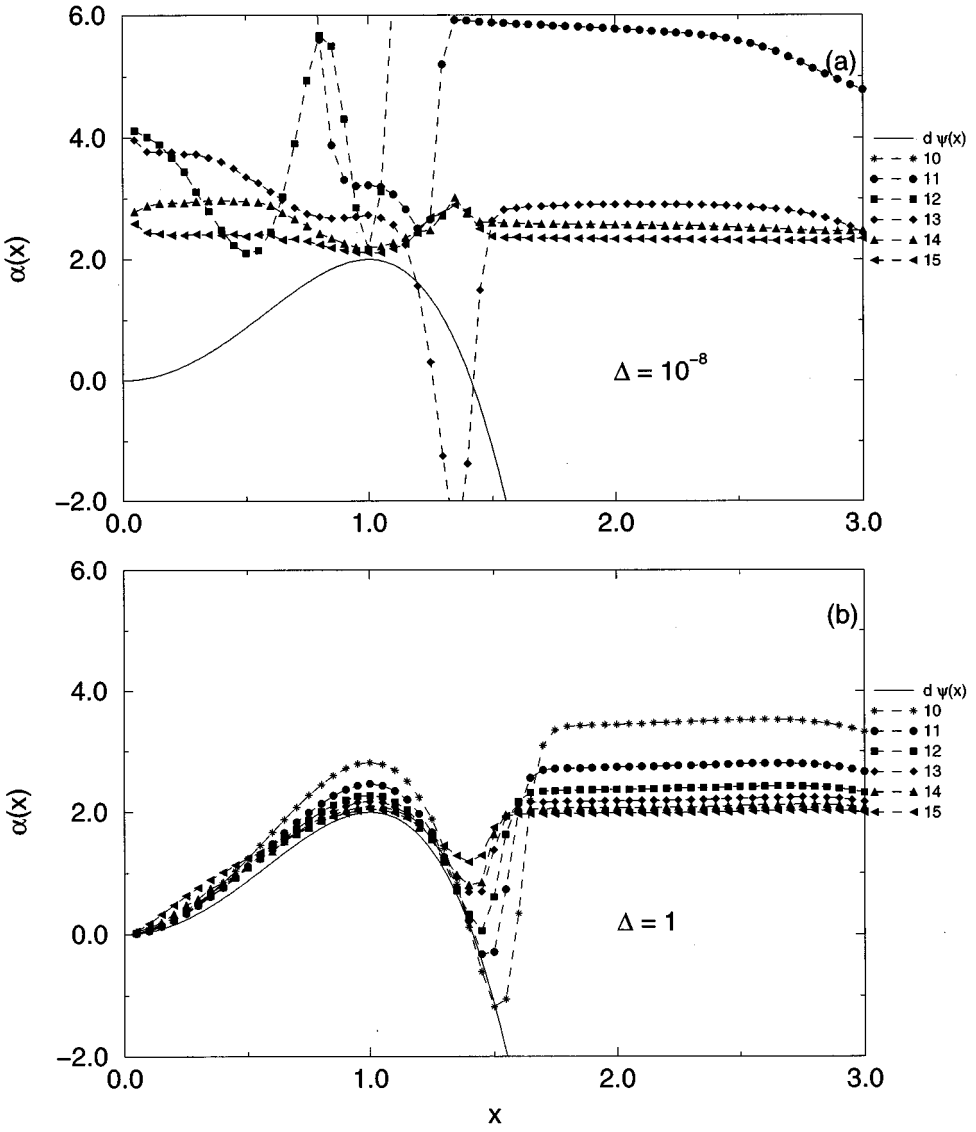

FIG. 12. Evolution of $\alpha(x)$ for the solution of the Bray-Humayun model with $N=100$, $d=2$, and $T_F=0$: (a) small initial fluctuations and (b) large initial fluctuations. Different curves refer to a sequence of time intervals growing exponentially with the label.

The asymptotic behavior is analytically accessible and it has been derived in detail in Ref. [10]. For quenches to $T_F \leqslant T_c$ with a NCOP, the long-time behavior is given by

$$C_0(\vec{k},t)=\Delta L^{\omega} f_0(x), \tag{46}$$

$$C_T(\vec{k},t)=T_F L^2 f_T(x), \tag{47}$$

with $L(t)=t^{1/2}$, $x=kL$, and

$$\omega=\begin{cases} 4-d & \text{for } T_F=T_c \\ d & \text{for } T_F<T_c, \end{cases} \tag{48}$$

$$f_0(x)=e^{-x^2}, \tag{49}$$

$$f_T(x)=\int_0^1 dy(1-y)^{-\omega/2}e^{-x^2 y}. \tag{50}$$

Notice that both contributions are in the scaling form (1) with $C_T(\vec{k},t)$ dominating in the quenches to T_c, while $C_0(\vec{k},t)$ dominates for $T_F<T_c$. One may go one step further regarding the order parameter as the sum of two contributions $\vec{\phi}=\vec{\sigma}+\vec{\zeta}$ whose correlations account for the two pieces in the structure factor $C_0(\vec{k},t)=\langle \sigma_\beta \sigma_\beta \rangle, C_T(\vec{k},t)=\langle \zeta_\beta \zeta_\beta \rangle$, and $\langle \sigma_\beta \zeta_\gamma \rangle = 0$. Therefore, for $T_F<T_c$ a sort of two-fluid picture of the quench is obtained, with the condensate $\vec{\sigma}$ and the thermal fluctuations $\vec{\zeta}$ having a distinct individuality due to the different scaling properties. Notice that the irrelevance of the thermal fluctuations is due to $\vec{\sigma}$ dominating $\vec{\zeta}$ and obeying the zero-temperature equation of motion.

With a COP there is additional structure since the thermal contribution itself contains two different pieces

$$C_T(\vec{k},t)=\begin{cases} C_<(\vec{k},t) & \text{for } k<x^* k_m(t) \\ C_>(\vec{k},t) & \text{for } k>x^* k_m(t), \end{cases} \tag{51}$$

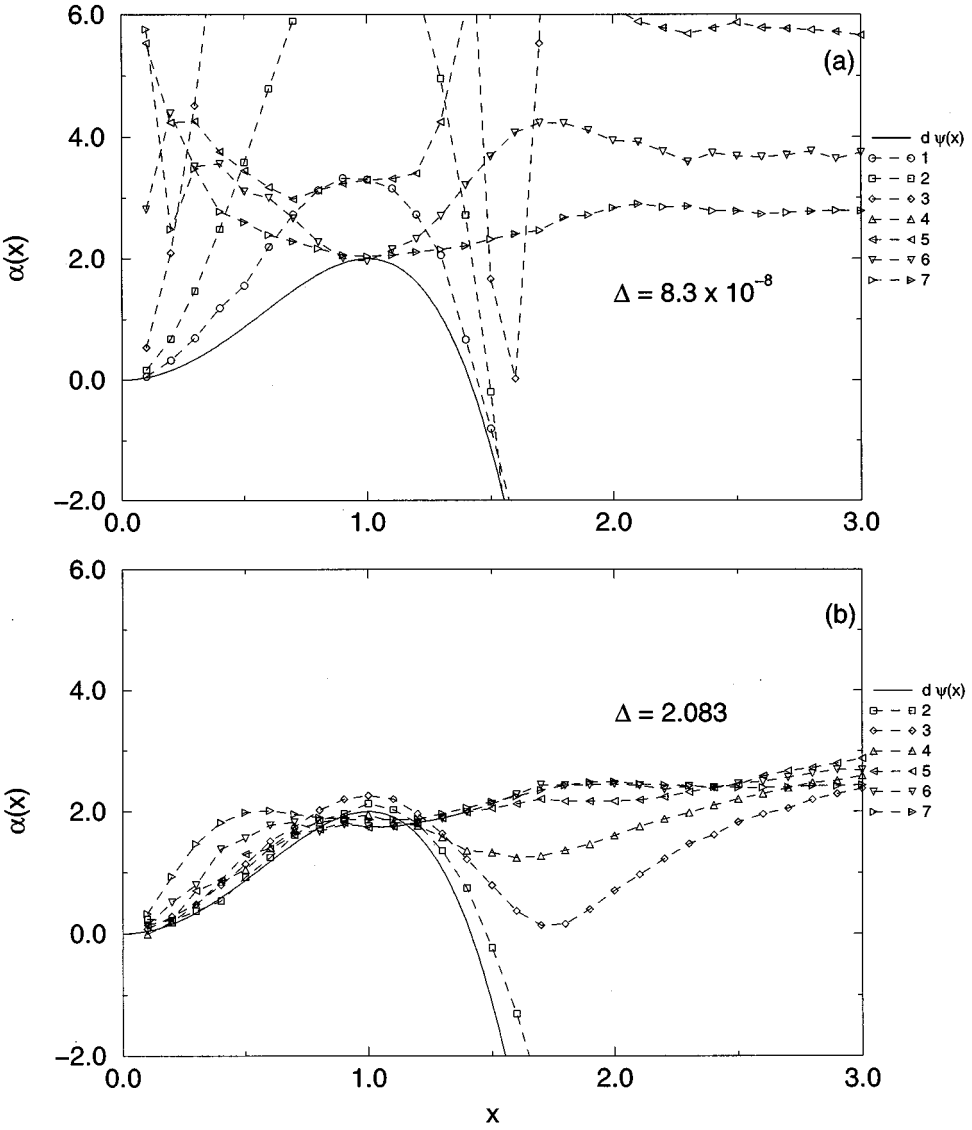

FIG. 13. Evolution of $\alpha(x)$ obtained in Ref. [14] by simulation of a system with $N=1$, $d=2$, and $T_F=0$: (a) small initial fluctuations and (b) large initial fluctuations. Different curves refer to a sequence of time intervals growing exponentially with the label.

with the asymptotic behaviors

$$C_0(\vec{k},t)=\Delta L^{\rho\psi(x)}, \tag{52}$$

$$C_<(\vec{k},t)=\frac{T_F}{x^2}L^{2+\rho\psi(x)}, \tag{53}$$

$$C_>(\vec{k},t)=\frac{T_F}{x^2}L^2, \tag{54}$$

$$\rho=\begin{cases} 0 & \text{for } T_F=T_c \\ d-2 & \text{for } 0<T_F<T_c \\ d & \text{for } T_F=0. \end{cases} \tag{55}$$

For simplicity, in writing Eqs. (52)–(54) we have neglected the logarithmic difference between $L(t)$ and $k_m(t)$, setting $x=kL$ and $L(t)=t^{1/4}$. New behavior arises in the region $0<T_F<T_c$, where there is a sharp distinction between what happens for $x<x^*$ and for $x>x^*$. In the first case $C_<(\vec{k},t)$ dominates over $C_0(\vec{k},t)$, while in the second case $C_>(\vec{k},t)$ dominates over $C_0(\vec{k},t)$. Therefore, with a COP we are led to regard the order parameter as the sum of three contributions $\vec{\phi}=\vec{\sigma}+\vec{\zeta}_<+\vec{\zeta}_>$, which again are characterized by distinct scaling properties and whose correlations are responsible, respectively, for $C_0(\vec{k},t)$, $C_<(\vec{k},t)$, and $C_>(\vec{k},t)$. The remarkable qualitative difference with the NCOP case is that now the condensate also is of thermal origin because the Bragg peak is formed by $\vec{\zeta}_<$. Hence the temperature is not an irrelevant variable. Furthermore, the thermal fluctuations $\vec{\zeta}_>$ that obey standard scaling as time goes on propagate from the large wave vectors toward the small wave vectors, following a pattern that is important, as we shall see below, for understanding what happens in the realistic systems. Finally, the $\vec{\sigma}$ contribution that was responsible for the condensate with a NCOP here is subdominant, but it can give rise to interesting preasymptotic behaviors if Δ and T_F are appropriately chosen.

In the numerical study of the structure factor, we shall devote particular attention to the transition from preasymptotic to asymptotic features. This we do both for the NCOP and COP with $d=3$ and $d=2$. Parameters of the quench are the final temperature T_F and the strength Δ of the fluctuations in the initial state (15). In particular, we will consider the two cases $\Delta=0$ (small Δ) and $\Delta=-r/g$ (large Δ), where $\sqrt{-r/g}$ is the equilibrium value of the order parameter at zero temperature. The final temperature of the quench is important in two respects. First of all, for $T_F>T_c$ the correlation length ξ is finite, while for $T_F\leqslant T_c$ it is infinite. This is important because the general structure of the time evolution is determined by the relation between a microscopic length L_0 and the correlation length ξ in the final equilibrium state. The initial fast transient, with no scaling, lasts up to some time t_0. At this point equilibrium is established over the length scale L_0 and if this is of the order of magnitude of ξ, final equilibrium is reached over the whole system as well. Instead, if $\xi\gg L_0$, a second regime is entered [17], during which the scaling relations (1) and (2) hold. This lasts up to the time t_1 such that $L(t_1)\simeq\xi$, when global equilibrium is again established. Clearly, if ξ is infinite, equilibrium is never reached and the scaling regime lasts forever. The second important feature involving the final temperature is that, while for $T_F\geqslant T_c$ only the thermal fluctuations grow, for $T_F<T_c$ there is growth of both the condensate and thermal fluctuations.

A. Multiscaling analysis

The interplay of all these elements produces a rich variety of behaviors that can be efficiently monitored through the multiscaling analysis. This works as follows. Let us assume that the structure factor can be written in the general multiscaling form

$$C(\vec{k},t)=[\mathcal{L}_1(t)]^{\alpha(x)}F(x), \tag{56}$$

with $x=k\mathcal{L}_2(t)$ and $\mathcal{L}_1(t)$ and $\mathcal{L}_2(t)$ two lengths. The functions $\alpha(x)$ and $F(x)$ are to be determined. In order to check on the assumption, the time axis is divided in intervals $(t_i,t_i+\tau_i)$, which in practice may also be of variable length τ_i, and within each interval the logarithm of $C(\vec{k},t)$ is plotted against the logarithm of $\mathcal{L}_1(t)$ for a fixed value of x. By measuring the slope and the intercept of the plot $\alpha(x,t_i)$ and $F(x,t_i)$ are obtained. The procedure is then repeated for different values of x and over different time intervals. If $\alpha(x,t_i)$ and $F(x,t_i)$ do not depend on t_i the assumption (56) is correct and scaling holds. Specifically, standard scaling is the case where $\mathcal{L}_1(t)=\mathcal{L}_2(t)$ and $\alpha(x)$ does not depend on x. In the case of multiscaling $\alpha(x)$ does depend on x and the two lengths $\mathcal{L}_1(t)$ and $\mathcal{L}_2(t)$ differ by a logarithmic factor. Conversely, if $\alpha(x,t_i)$ and $F(x,t_i)$ do depend on t_i, scaling does not hold. Notice that in the case that equilibrium has been reached, the disappearance of the time dependence shows up as $\alpha(x,t_i)\equiv 0$. In the following we shall not be interested in the determination of $F(x)$ and we shall concentrate on $\alpha(x)$.

As an example, consider the quench to $T_F=0$. With a NCOP the exact form of the structure factor is given by [8]

$$C(\vec{k},t)=\Delta\exp\{-[Q(t)+(kL)^2]\}, \tag{57}$$

where $Q(t)$ is a function of time and $L(t)=t^{1/2}$. Hence we have the natural choice $\mathcal{L}_2(t)=L(t)$ and, using Eq. (56),

$$\alpha(x,t)=-\frac{Q(t)}{\ln\mathcal{L}_1(t)}, \tag{58}$$

which shows that if there is scaling it is of the standard type. This occurs for long times, where $Q(t)=-d\ln L(t)$ suggests to take $\mathcal{L}_1(t)=\mathcal{L}_2(t)=L(t)$, yielding $\alpha(x,t)=d$. Conversely, for short times, if Δ is small enough to allow for the application of the linear approximation, we have $Q(t)=2rt$ and there is no scaling since the time dependence does not drop out

$$\alpha(x,t)=-\frac{2rt}{\ln L(t)}. \tag{59}$$

With a COP instead, the exact form of the structure factor is given by [8]

$$C(\vec{k},t)=\Delta\exp(k_mL)^4\psi(k/k_m), \tag{60}$$

where $k_m(t)$ is the peak wave vector, $L(t)=t^{1/4}$, and ψ is given by Eq. (9). Choosing $\mathcal{L}_2(t)=k_m^{-1}(t)$, we find

$$\alpha(x,t)=\frac{[k_m(t)L(t)]^4\psi(x)}{\ln\mathcal{L}_1(t)}, \tag{61}$$

which shows that the x dependence cannot be eliminated and therefore that scaling can only be of the multiscaling type. This occurs for long times with $\mathcal{L}_1(t)=(k_m^{2-d}L^2)^{1/d}$, yielding

$$\alpha(x,t)=d\psi(x). \tag{62}$$

Using Eq. (11), the two lengths $\mathcal{L}_1(t)$ and $\mathcal{L}_2(t)$ are related by $\mathcal{L}_1(t)/\mathcal{L}_2(t)\sim(\ln L)^{2/d}$. Conversely, in the very early stage where the linear approximation holds $\mathcal{L}_2(t)=k_m^{-1}=\sqrt{-2/r}$ is time independent and $\mathcal{L}_1\sim t^{1/2d}$, yielding

$$\alpha(x,t)\sim\frac{t}{\ln t}\psi(x), \tag{63}$$

which displays the absence of scaling through a time-dependent prefactor in front of $\psi(x)$.

B. Evolution of $\alpha(x,t)$

In the following we illustrate the evolution of $\alpha(x,t)$ obtained numerically over a sequence of time intervals, with $r=-1$ and $g=1$.

1. NCOP d=3

Let us begin with a NCOP in three dimensions. The critical temperature is finite $T_c=2\pi$ and the exponent α is obtained setting $\mathcal{L}_1(t)=\mathcal{L}_2(t)$ and extracting this length from the inverse of the halfwidth of the structure factor. According to the general outline presented at the beginning of this section, we expect to detect the establishment of equilibrium for $T_F>T_c$ through the vanishing of α and the scaling behavior lasting indefinitely for $T_F\leqslant T_c$, through the disappearance of the time dependence around a nonvanishing value of α. This is clearly illustrated in Fig. 3, where α is plotted for a quench

well above T_c with $T_F=20$ and for a quench to T_c. In the first case the lines rapidly collapse on $\alpha=0$, while in the second case the collapse is on $\alpha=2$. It is then interesting to consider the case of a final temperature slightly above T_c, which corresponds to a large but finite ξ. Also in this case α is expected to collapse eventually on $\alpha=0$; however, as long as $L(t)$ is large but smaller than ξ, one expects to observe a behavior similar to the one in the quench to T_c. Indeed, this is what happens in Fig. 4(a), obtained by plotting α for $T_F=6.35$. After the initial transient there is a collapse on $\alpha=2$, revealing critical scaling. However, this does not last indefinitely as in the case of the quench to T_c, but it lasts for the time necessary for $L(t)$ to catch up with ξ. After this a new transient sets in and the eventual collapse on the equilibrium value $\alpha=0$ takes place. For $T_F<T_c$ the behavior of α is quite similar to the one for $T_F=T_c$, since in both cases $\xi=\infty$. The only difference is that the asymptotic behavior produces collapse on the value $\alpha=d=3$. For T_F slightly below T_c, e.g., $T_F=6.20$ in Fig. 4(b), there is crossover from critical scaling with $\alpha=2$ to the final value with $\alpha=3$. In general, the asymptotic behavior for $0<T_F<T_c$ and $T_F=0$ is the same (Fig. 5), confirming the irrelevance of thermal fluctuations. In all quenches considered, the variation of the size Δ of initial fluctuations does not produce significant differences.

2. NCOP d=2

In two dimensions the critical temperature (26) vanishes. So, for any $T_F>0$ one should observe a behavior for α similar to the one obtained with $d=3$ and $T_F>T_c$. This is the case for quenches with a final temperature well above zero, where behaviors of α very close to the one in Fig. 3(a) are obtained. Similarly, for the quench to $T_F=0$ the same behavior as in Fig. 5(b) is obtained, except that now the lines collapse on $\alpha=d=2$.

A case to be considered separately is when T_F is finite but very close to zero. Figure 6, corresponding to $T_F=0.3$ and $T_F=10^{-6}$, displays an intermediate scaling behavior with $\alpha=2$ preceding the eventual collapse on the equilibrium value $\alpha=0$. At first sight this looks like the behavior of Fig. 4(a) in the quench to a final temperature slightly above T_c. However, the interpretation is more subtle since what is growing here, as long as $L(t)<\xi$, are not the critical fluctuations but the condensate. The distinction between condensation and critical behavior is actually impossible to make with a NCOP on the basis of the value of α since with $d=2$ in both cases $\alpha=2$. This remark will become clear with a COP because in that case the growth of the critical fluctuations is associated with standard scaling, while the growth of the condensate gives rise to multiscaling.

3. COP d=3

We now move on to the case of a COP with both small and large initial fluctuations. As discussed above, $\alpha(x,t)$ is extracted by defining $x=k/k_m$, where $k_m(t)$ is the peak wave vector, and plotting $\ln C$ vs $\ln\mathcal{L}_1(t)$ with $\mathcal{L}_1(t)=(k_m^{2-d}L^2)^{1/d}$ and $L(t)=t^{1/4}$. For quenches to $T_F\geqslant T_c$ the behavior of $\alpha(x,t)$ essentially follows the same pattern as in the NCOP case. Apart from some differences in the time-dependent transients, again for $T_F>T_c$ and for $T_F=T_c$ curves collapse, respectively, on $\alpha=0$ and $\alpha=2$. In Fig. 7 we illustrate what happens in the quench slightly above [Fig. 7(a)] and slightly below [Fig. 7(b)] T_c. In both cases there is a preasymptotic standard scaling behavior with $\alpha=2$ due to the critical point in the neighborhood, followed by the incipient crossover toward the asymptotic behavior. Above T_c this is $\alpha=0$, as revealed by α deviating downward, while below T_c the deviation occurs upwardly, for $x<x^*$, toward the asymptotic form of Fig. 1.

Where the difference between the NCOP and COP becomes remarkably evident is in the quenches well below T_c. Let us first consider (Fig. 8) $T_F=0$. After a time-dependent transient [Fig. 8(a)], which for small Δ in the early stage is well described by Eq. (63), the curves of $\alpha(x,t)$ collapse [Fig. 8(b)] on the limiting curve (62) depicted in Fig. 1. Instead, for $T_F=1$ (Fig. 9), the collapse occurs on the finite-temperature asymptotic form of Fig. 1, with minor differences in the transient due to the size of Δ. However, going to a temperature much lower but finite (Fig. 10), while for $\Delta=0$ [Fig. 10(a)] α follows the same pattern as in Fig. 9, the behavior in Fig. 10(b) with $\Delta=1$ is drastically different. What we have here is multiscaling as in the quench to $T_F=0$ for $x<x^*$ and standard scaling with $\alpha=2$ for $x>x^*$. All these features can be accounted for on the basis of the discussion made at the beginning of this section. As long as T_F is sufficiently large or Δ small, as in Figs. 9 and 10(a), only $C_<(\vec{k},t)$ and $C_>(\vec{k},t)$ contribute to $\alpha(x,t)$ producing the characteristic behavior of Fig. 1. However, when Δ is finite and T_F small enough, there can be a sizable interval of time during which $C_0(\vec{k},t)$ dominates over $C_<(\vec{k},t)$, for $x<x^*$, producing the scaling pattern in Fig. 10(b). This behavior is preasymptotic and eventually the crossover to the pattern of Fig. 9 takes place as $C_<(\vec{k},t)$ grows large enough to overtake $C_0(\vec{k},t)$. In our numerical solution the computation was not run long enough to actually detect this crossover, but it is clear that by modulating the parameters of the quench Δ and T_F the crossover time can be varied at will.

4. COP d=2

It is now interesting to see how this variety of behaviors is affected by pushing the critical temperature to zero in two dimensions. The difference with respect to the previous case is that now the line of fixed points in between $T_F=0$ and T_c has disappeared and with it, supposedly, also the associated asymptotic behavior. Actually, only the fixed point at $T_F=0$ has survived. Thus we should observe either the relaxation to equilibrium for $T_F>0$ or the multiscaling behavior for $T_F=0$. Indeed, for temperatures such as $T_F=10$ the collapse on $\alpha=0$ is observed. Similarly, the quench to $T_F=0$ produces a behavior identical to the one in Fig. 8, except that the peak value of α is given by 2 in place of 3. The interesting differences arise when quenches to small but finite T_F are considered. In fact, when T_F is low ξ is large and an intermediate scaling regime preceding the final equilibration is expected. The question is what it will be like. For $T_F=10^{-6}$ (Fig. 11) and $\Delta=0$ there is standard scaling with $\alpha=2$, while for $\Delta=1$ the pattern is identical to the one in Fig. 10(b), except for the obvious modification $\alpha(x=1)=d=2$. The first observation is that these are preasymptotic behaviors since eventually α must vanish. The second is that this

phenomenology can be understood regarding, as long as $L(t)<\xi$, the structure factor as made up of the three contributions (52)–(54). Namely, as long as $L(t)<\xi$, there is growth of the condensate and of thermal fluctuations, as in the quench below the critical point. Thermal fluctuations are clearly due to $T_F>0$, while the growth of the condensate originates from the underlying fixed point being at $T_F=0$. The net result is that the intermediate scaling behavior with $\Delta=0$ is due to $C_<(\vec{k},t)$ and $C_>(\vec{k},t)$, which scale both like L^2 since ρ vanishes when $d=2$. Instead, with $\Delta=1$ we are confronted again with a situation where, in the time of the computation, $C_0(\vec{k},t)$ dominates over $C_<(\vec{k},t)$ producing the pattern of Fig. 11(b). As a matter of fact, this is a pre-preasymptotic scaling behavior, since when $C_<(\vec{k},t)$ overtakes $C_0(\vec{k},t)$ a behavior of the type in Fig. 11(a) is expected to occur before the eventual relaxation to a vanishing α.

IV. CONCLUSION

In this paper we have investigated the origin of the noncommutativity of the limits $t\to\infty$ and $N\to\infty$ in the dynamics of the first-order transitions. The main result is that when the $N\to\infty$ limit is taken first the underlying phase transition, which we have called condensation, is qualitatively different from the usual process of ordering obtained with the limits in the opposite order. In particular, condensation in conjunction with a COP gives rise, for reasons that are not yet clear, to two phenomena that are strikingly different from what one has in phase ordering, namely, (i) multiscaling and (ii) relevance of the thermal fluctuations. We then proceeded to an extensive investigation of the scaling properties of the structure factor in the large-N model for quenches to a final temperature greater than, equal to, or lower than T_c. We have found a rich variety of behaviors, which can be studied in great detail through the multiscaling analysis. Particularly interesting is the existence of preasymptotic scaling, which can be explained through the competition between different components of the order parameter with distinct scaling properties.

Even though it is quite clear that the large-N model is not perturbatively close to the phase-ordering processes in realistic systems, in concluding the paper we wish to elaborate on the connections that nonetheless exist. In order to do this we use the Bray-Humayun (BH) model [11] as an intermediate step. As mentioned above, in this model the structure factor for the quenches to $T_F=0$ with a COP displays standard scaling for any finite value of N. The discussion in Sec. III on the behavior of α in the quenches to $T_F=10^{-6}$ helps to understand how this comes about. By integrating formally the equation of motion, the BH structure factor can be written as the sum of two contributions

$$C(\vec{k},t)=C_0(\vec{k},t)+C_N(\vec{k},t), \tag{64}$$

where $C_0(\vec{k},t)$ is given by Eq. (44), while

$$C_N(\vec{k},t)=-\frac{2}{N}k^p\int_0^t dt' R(t')\frac{C_0(\vec{k},t)}{C_0(\vec{k},t')}D(\vec{k},t'), \tag{65}$$

with

$$D(\vec{k},t)=\int\frac{d^dk_1}{(2\pi)^d}\frac{d^dk_2}{(2\pi)^d}C(\vec{k}-\vec{k}_1,t)C(\vec{k}_1-\vec{k}_2,t)C(\vec{k}_2,t), \tag{66}$$

contains the nonlinearity and $R(t)$ is given by Eqs. (28) and (29) [14]. Although Eq. (43) refers to a quench to $T_F>0$ with $N=\infty$ and Eq. (64) to a quench to $T_F=0$ and N finite, the mechanism regulating the competition between the two terms is the same. In particular, in both cases $C_0(\vec{k},t)$ can compete with the second term only for $x<x^*$. Bray and Humayun have shown that $C_N(\vec{k},t)$ asymptotically obeys standard scaling with $\alpha=d$. It is then clear that by choosing Δ and N properly there may be a preasymptotic regime during which $C_0(\vec{k},t)$ dominates for $x<x^*$, much in the same way as in Sec. III $C_0(\vec{k},t)$ was found to dominate over $C_T(\vec{k},t)$. Here $1/N$ plays a role similar to that of T_F and the crossover time depends on both Δ and N [11,14]. With $N=100$ and $d=2$ (Fig. 12) a behavior for $\alpha(x,t)$ is obtained that is practically the same of that in Fig. 11. In order to complete the picture, we reproduce in Fig. 13 the behavior of $\alpha(x,t)$ for the scalar system obtained in Ref. [15] by the simulation of Eq. (12) with $N=1$ and $d=2$. Again the same pattern is found, revealing that the same mechanism is operating also in this case. Therefore, one may conclude that the behavior of the large-N model associated with $C_0(\vec{k},t)$ describes what happens in the preasymptotic regime also in the phase-ordering processes over the shrinking range of wave vectors with $k<x^*k_m(t)$. In other words, the asymptotic regime is preceded by a time regime where phase ordering over the short length scale seems to coexist with condensation over the large length scale. This is not surprising for a NCOP since correlations are established over regions of size $L(t)$ and the statistics can be expected to become Gaussian over distances larger than $L(t)$. For a COP it is less straightforward, although the occurrence of Gaussian statistics on large length scales can be detected much more easily through the appearance of multiscaling behavior.

APPENDIX A

From Eq. (1) the real-space scaling form of the correlation function is given by

$$G(\vec{r},t)=r^{\alpha-d}g(r/L(t)), \tag{A1}$$

where $g(x)$ is the scaling function and $g(0)$ is a finite quantity. For $r\ll L(t)$ Eq. (A1) gives the equilibrium decay of the correlation function

$$G_{eq}(\vec{r})\sim r^{\alpha-d}. \tag{A2}$$

On the other hand, the correlation function on a fractal [18] decays as

$$G_{eq}(\vec{r})\sim r^{2(D-d)}, \tag{A3}$$

where D is the fractal dimensionality. Comparing Eq. (A3) with Eq. (A2), the fractal dimensionality of the correlated regions is given by $D=\frac{1}{2}(\alpha+d)$ and using Eq. (3),

$$D=\begin{cases}\frac{1}{2}(2+d-\eta) & \text{for } T_F=T_c \\ d & \text{for } T_F<T_c\,.\end{cases} \tag{A4}$$

APPENDIX B

1. NCOP

Equation (37) can be rewritten as

$$\xi^{-2}=r+gT_FB(0)+\frac{gT_F}{V\xi^{-2}}+gT_F[B(\xi^{-2})-B(0)] \tag{B1}$$

and using $r+gT_cB(0)=0$,

$$\frac{\xi^{-2}}{g}=c+T_F[B(\xi^{-2})-B(0)], \tag{B2}$$

where

$$c=-\frac{r}{g}\left(\frac{T_F-T_c}{T_c}\right)+\frac{T_F}{V\xi^{-2}}. \tag{B3}$$

Since $[B(\xi^{-2})-B(0)]$ is a nonpositive monotonical decreasing function, there is a positive solution of Eq. (B2) for $c>0$, a vanishing solution for $c=0$, and no solution for $c<0$. For $T_F<T_c$ the quantity c cannot be positive because in that case ξ^{-2} would be positive and the second term on the right-hand side of Eq. (B3) would vanish in the infinite-volume limit, producing $c<0$. Therefore, c can only vanish, implying

$$\lim_{V\to\infty}\frac{T_F}{V\xi^{-2}}=\gamma^2=-\frac{r}{g}\left(\frac{T_c-T_F}{T_c}\right). \tag{B4}$$

2. COP

With a conserved order parameter, Eq. (36) is replaced by

$$\xi^{-2}=r+\frac{gT_F}{V}\sum_{k\neq 0}\frac{1}{k^2+\xi^{-2}}, \tag{B5}$$

which allows for a solution $\xi^{-2}>-k_{min}^2$, where $k_{min}\sim V^{-1/d}$ is the minimum value of the wave vector. For

$$T_F<\tilde{T}_c=-\frac{r}{g}\left[\frac{1}{V}\sum_{k\neq 0}\frac{1}{k^2}\right]^{-1} \tag{B6}$$

the solution is negative $-k_{min}^2<\xi^{-2}<0$. In the infinite volume limit $\tilde{T}_c\to T_c$ and $\xi^{-2}\to -k_{min}^2$. Thus, rewriting Eq. (B5) as

$$\xi^{-2}=r+gT_FB(\xi^{-2})+\frac{gT_F}{V(k_{min}^2+\xi^{-2})}, \tag{B7}$$

we can analyze this equation exactly as in the NCOP case, obtaining for $T_F<T_c$ the analog of Eq. (B4)

$$\lim_{V\to\infty}\frac{T_F}{V(k_{min}^2+\xi^{-2})}=\gamma^2=-\frac{r}{g}\left(\frac{T_c-T_F}{T_c}\right). \tag{B8}$$

[1] For a review see A. J. Bray, Adv. Phys. **43**, 357 (1994).

[2] The formal structure for this program can be found in G. F. Mazenko, O. T. Valls, and M. Zannetti, Phys. Rev. B **38**, 520 (1988).

[3] H. K. Janssen, B. Schaub, and B. Schmitt, Z. Phys. B **73**, 539 (1989); H. K. Janssen, in *From Phase Transitions to Chaos*, edited by G. Gyorgyi, I. Kondor, L. Sasvari, and T. Tèl (World Scientific, Singapore, 1992), p. 68.

[4] J. W. Cahn and J. E. Hilliard, J. Chem. Phys. **31**, 688 (1959).

[5] T. Ohta, D. Jasnow, and K. Kawasaki, Phys. Rev. Lett. **49**, 1223 (1982); G. F. Mazenko, Phys. Rev. B **42**, 4487 (1990); **43**, 5747 (1991). The Gaussian auxiliary field approximations are critically reviewed in C. Yeung, Y. Oono, and A. Shinozaki, Phys. Rev. E **49**, 2693 (1994).

[6] K. R. Elder, T. M. Rogers, and R. C. Desai, Phys. Rev. B **38**, 4725 (1988); J. S. Langer, in *Solids Far from Equilibrium*, edited by C. Godrèche (Cambridge University Press, Cambridge, 1992).

[7] A. J. Bray and K. Humayun, Phys. Rev. E **48**, R1609 (1993); S. De Siena and M. Zannetti, *ibid.* **50**, 2621 (1994); G. F. Mazenko, *ibid.* **49**, 3717 (1994); **50**, 3485 (1994).

[8] A. Coniglio and M. Zannetti, Europhys. Lett. **10**, 575 (1989).

[9] G. F. Mazenko and M. Zannetti, Phys. Rev. B **32**, 4565 (1985).

[10] A. Coniglio, P. Ruggiero, and M. Zannetti, Phys. Rev. E **50**, 1046 (1994).

[11] A. J. Bray and K. Humayun, Phys. Rev. Lett. **68**, 1559 (1992).

[12] T. H. Berlin and M. Kac, Phys. Rev. **86**, 821 (1952).

[13] H. W. Lewis and G. H. Wannier, Phys. Rev. **88**, 682 (1952); **90**, 1131(E) (1953).

[14] C. Castellano and M. Zannetti, Phys. Rev. E **53**, 1430 (1996).

[15] C. Castellano and M. Zannetti, Phys. Rev. Lett. **77**, 2742 (1996).

[16] For a comparative discussion of the two models see M. Kac and C. J. Thompson, J. Math. Phys. (N.Y.) **18**, 1650 (1977).

[17] G. F. Mazenko, Phys. Rev. B **26**, 5103 (1982).

[18] T. Vicsek, *Fractal Growth Phenomena* (World Scientific, Singapore, 1989).